

Redox Properties of Porphycenes and Metalloporphycenes. A Comparison with Porphyrins

C. Bernard,[†] J. P. Gisselbrecht,[†] M. Gross,^{*†} E. Vogel,^{*‡} and M. Lausmann[‡]

Laboratoire d'Electrochimie et de Chimie Physique du Corps Solide, Université Louis Pasteur, URA au CNRS No. 405, 4, rue Blaise Pascal, 67000 Strasbourg, France, and Institut für Organische Chemie, Universität Köln, Greinstrasse 4, D 5000 Köln 41, Germany

Received May 19, 1993*

An electrochemical analysis of a series of porphycenes and metalloporphycenes in tetrahydrofuran, *N,N*-dimethylformamide, and dichloromethane is reported. This analysis combined the use of polarographic, steady-state voltammetric, cyclic voltammetric, and spectroelectrochemical methods. The free-base porphycenes studied were porphycene (H₂Pc), 2,3,6,7,12,13,16,17-octaethylporphycene (H₂OEPc), 2,7,12,17-tetra-*n*-propylporphycene (H₂TPrPc), and its tetrabromo derivative 3,6,13,16-tetrabromo-2,7,12,17-tetra-*n*-propylporphycene (H₂TBrTPrPc), respectively. Each free-base and nickel porphycene was found to undergo two reversible one-electron reductions as well as two oxidations all centered on the tetrapyrrolic ring system. CoTPrPc was reduced in two one-electron steps and oxidized in three one-electron redox processes. The reductions were assigned as occurring on the tetrapyrrolic ligand while the first oxidation step was ascribed to a Co(II) to Co(III) redox process. (Fe^{III}TPrPc)Cl was reduced in three steps, and it was oxidized in two one-electron steps. The first of these reduction processes was clearly metal centered [Fe(III) → Fe(II)]. All four other electron transfers were ligand centered. The corresponding iron μ -oxo dimer (Fe^{III}TPrPc)₂O underwent four one-electron oxidations as well as four one-electron reductions. The studies reported herein indicate that porphycenes, structural isomers of porphyrins, behave electrochemically much like bacteriochlorins: only two reduction steps are observed in the available potential range, and as compared to those of the porphyrins, smaller potential differences are seen between the first oxidation and the first reduction waves.

The porphycenes, synthesized from 5,5'-diformyl- (or 5,5'-diacyl-) 2,2'-bipyrrroles by reductive coupling with low-valent titanium (Mc Murry reaction), are the only tetrapyrrolic porphyrin structural isomers presently known.^{1,2} Not surprisingly, this fascinating new set of molecules is attracting considerable interest. While the physical chemistry and specifically the electrochemical behavior of the porphyrins have been extensively explored,^{3–8} studies of the redox behavior^{9,10} and physicochemical^{11–17} properties of porphycenes are still relatively scarce.

The present paper deals with the redox characteristics of porphycenes. Four free-base porphycene derivatives were studied: H₂Pc (Pc = porphycene), H₂TPrPc (2,7,12,17-tetra-*n*-propylporphycene), H₂OEPc (2,3,6,7,12,13,16,17-octaethylporphycene), H₂TPrTBrPc (3,6,13,16-tetrabromo-2,7,12,17-tetra-*n*-propylporphycene). Several metalloporphycenes were also investigated electrochemically. These include the following: NiOEPc, NiTPrPc, NiTPrPc-9,10,19,20 (TPrPc-9,10,19,20 is 9,10,19,20-tetra-*n*-propylporphycene), CoTPrPc, FeClTPrPc, and the dinuclear μ -oxo species (FeTPrPc)₂O. The structures of these systems are shown in Figure 1.

[†] Université Louis Pasteur.[‡] Universität Köln.* Abstract published in *Advance ACS Abstracts*, April 15, 1994.

- (1) Vogel, E.; Köcher, M.; Schmickler, H.; Lex, J. *Angew. Chem., Int. Ed. Engl.* **1986**, *25*, 257–259.
- (2) Vogel, E.; Balci, M.; Pramod, K.; Koch, P.; Lex, J.; Ermer, O. *Angew. Chem., Int. Ed. Engl.* **1987**, *26*, 928–931.
- (3) Felton, R. H. In *The Porphyrins* Dolphin, D., Ed.; Academic: New York, 1978; Vol. 5, Chapter 3, pp 53–125.
- (4) (a) Boucher, L. J. *Coord. Chem. Rev.* **1972**, *7*, 289–329. (b) Kadish K. M. In *Progress in Inorganic Chemistry*; Lippard, S. J., Ed.; John Wiley & Sons: New York, 1986; Vol. 34, pp 435–605.
- (5) Guillard, R.; Lecomte, C.; Kadish, K. M. *Structure and Bonding*; Springer Verlag: Berlin, Heidelberg, 1987; Vol. 64, pp 205–268.
- (6) Fuhrhop, J.-H.; Kadish, K. M.; Davis, D. G. *J. Am. Chem. Soc.* **1973**, *95*, 5140–5147.
- (7) Giraudeau, A.; Callot, H. J.; Jordan, J.; Ezhar, I.; Gross M. *J. Am. Chem. Soc.* **1979**, *101*, 3857–3862.
- (8) Giraudeau, A.; Ezahr, I.; Gross, M.; Callot, H. J.; Jordan, J. *Bioelectrochem. Bioenerg.* **1976**, *3*, 519–527.
- (9) Renner, M. W.; Forman, A.; Wu, W.; Chang, C. K.; Fajer, J. *J. Am. Chem. Soc.* **1989**, *111*, 8618–8621.
- (10) Gisselbrecht, J. P.; Gross, M.; Köcher, M.; Lausmann, M.; Vogel, E. *J. Am. Chem. Soc.* **1990**, *112*, 8618–8620.
- (11) Ofir, H.; Regev, A.; Levanon, H.; Vogel, E.; Köcher, M.; Balci, M. *J. Phys. Chem.* **1987**, *91*, 2686–2688.
- (12) Levanon, H.; Toporowicz, M.; Ofir, H.; Fessenden, R. W.; Das, P. K.; Vogel, E.; Köcher, M.; Pramod, K. *J. Phys. Chem.* **1988**, *92*, 2429–2433.
- (13) (a) Schlüpmann, J.; Huber, M.; Toporowicz, M.; Köcher, M.; Vogel, E.; Levanon, H.; Möbius, K. *J. Am. Chem. Soc.* **1988**, *110*, 8566–8567. (b) Schlüpmann, J.; Huber, M.; Toporowicz, M.; Plato, M.; Köcher, M.; Vogel, E.; Levanon, H.; Möbius, K. *J. Am. Chem. Soc.* **1990**, *112*, 6463–6471.
- (14) Vogel, E. *Pure Appl. Chem.* **1990**, *62*, 557–564.
- (15) Wehrle, B.; Limbach, H. H.; Köcher, M.; Ermer, O.; Vogel, E. *Angew. Chem., Int. Ed. Engl.* **1987**, *26*, 934–936.

Experimental Section

All porphycenes and metalloporphycenes used in the present study were synthesized in accord with published procedures.^{1,2,13,18} Their electrochemistry was studied in three different solvent systems: *N,N*-dimethylformamide (DMF), tetrahydrofuran (THF), and dichloromethane (CH₂Cl₂). All three of these afforded acceptable porphycene solubility. DMF was purified as described previously¹⁹ and stored under argon. CH₂Cl₂ was dried over molecular sieves (4 Å), stored under argon, and distilled from CaH₂ before use. THF was purified by distillation from LiAlH₄ immediately before use. Tetraethylammonium perchlorate (TEAP) was used as the supporting electrolyte in DMF. It was recrystallized before use.²⁰ For the studies carried out in CH₂Cl₂ and in THF, tetrabutylammonium perchlorate (TBAP) was used as the supporting electrolyte. It was purified according to standard procedures.¹⁹

Tast polarographic and cyclic voltammetric measurements were carried out using a dropping mercury electrode with a PRG4 multipurpose electrochemical device (Soléa, Tacussel, France). The mercury flow for a 35-cm mercury column was $m = 0.65$ mg/s.

- (16) Oertling, W. A.; Wu, W.; Lopez-Garriga, J. J.; Kim, Y.; Chang, C. K. *J. Am. Chem. Soc.* **1991**, *113*, 127–134.
- (17) Waluk, J.; Müller, M.; Swiderek, P.; Köcher, M.; Vogel, E.; Hohlneicher, G.; Michl, J. *J. Am. Chem. Soc.* **1991**, *113*, 5511–5527.
- (18) (a) Vogel, E.; Köcher, M.; Lex, J.; Ermer, O. *Isr. J. Chem.* **1989**, *29*, 257–266. (b) Will, S.; Rahbar, A.; Schmickler, H.; Lex, J.; Vogel, E. *Angew. Chem., Int. Ed. Engl.* **1990**, *29*, 1390–1393.
- (19) El Jammal, A.; Graf E.; Gross, M. *Electrochim. Acta* **1986**, *11*, 1457–1465.
- (20) Callot, H. J.; Giraudeau, A.; Gross, M. *J. Chem. Soc., Perkin Trans. 2* **1975**, 1321–1324.

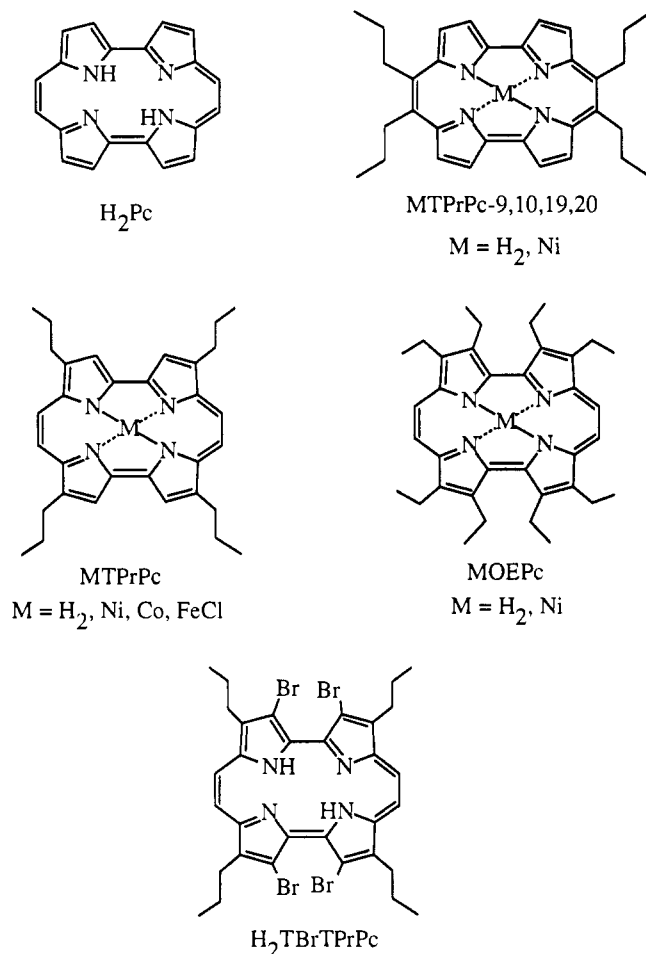


Figure 1. Porphyrines considered in this study.

The exhaustive reduction of the studied species was achieved either chemically with sodium amalgam as the reductant or electrochemically through controlled potential electrolysis; in the latter case, a small electrolysis cell (5 mL of electrolyte solution) was used and the working electrode was a coiled platinum wire with a large area (25 cm²). The auxiliary electrode was a platinum wire separated from the electrolysis cell by a glass frit of low porosity. The cell was connected to a potentiostat (Brucker model EI-30).

Steady-state voltammetry on a rotating disk electrode (RDE) and cyclic voltammetry with sweep rates ranging from 10 mV/s to 20 V/s were carried out on a computerized DACFAMOV electrochemical device (Microtec-CNRS, Toulouse, France) connected to an Apple II microcomputer. A classical three-electrode cell was used. The working electrode was either a platinum disk electrode (2-mm diameter, type EDI, Tacussel, France) or a glassy carbon electrode (GCE, 3-mm diameter). The auxiliary electrode was a platinum wire, and the reference electrode was an aqueous saturated calomel electrode. In our studies ferrocene was used as the internal standard. The Fc/Fc⁺ redox couple ($E_{1/2}$) was observed at +0.48 V/SCE in CH₂Cl₂ + 0.1 M TBAP, +0.49 V/SCE in DMF + 0.1 M TEAP, and +0.55 V/SCE in THF + 0.1 M TBAP, respectively.

Spectroelectrochemical experiments were carried out with a diode array spectrophotometer (8452 A, Hewlett Packard). The spectroelectrochemical cell was a home-made borosilicate glass cell having an optical pathway of about 0.1 mm. The optically transparent thin-layer electrode (OTTLE) was a platinum grid (1000 mesh) placed in the optical pathway. Under these conditions an exhaustive electrolysis was carried out in a few minutes (5 min) instead of 0.5 h for a large-scale electrolysis. As a result of this shorter time scale, further chemical reactions of the electrogenerated species were avoided or thwarted and spectral measurements were allowed on the species resulting from the electron-transfer reactions.

Results

Oxidation-Reduction of the Free-Base Porphyrines H₂Pc, H₂TPrPc, H₂OEPc, and H₂TPrTBrPc. The redox properties of

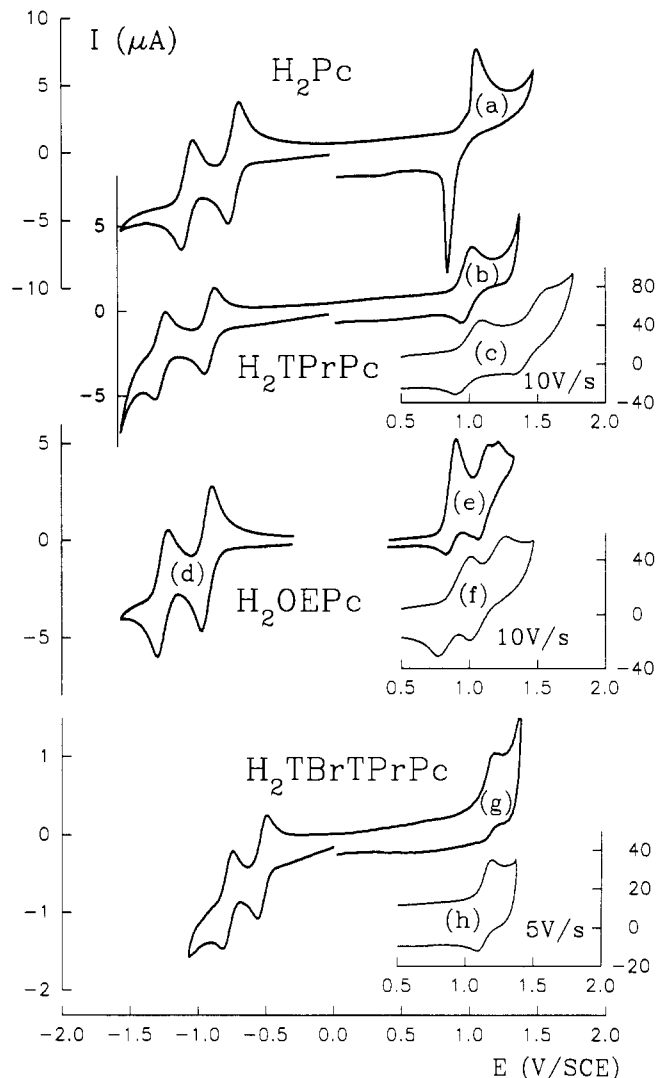


Figure 2. Cyclic voltammetry of free-base porphyrines on a Pt electrode in CH₂Cl₂ + 0.1 M TBAP. Scan rate: 0.1 V/s.

these four free-base porphyrines were investigated by cyclic voltammetry in three solvents, CH₂Cl₂, THF, and DMF. The electrochemical studies were mainly based on cyclic voltammetry. This technique was chosen because it allows for the detection of any chemical reaction(s) that might be associated with the charge transfer. When an electron transfer was followed by a chemical reaction (EC mechanism), we increased the scan rate so as to carry out measurements on a time scale where only the electron transfer had to be taken into account. This procedure then allowed the estimation of the formal potential of the charge transfer process $E^{\circ} = (E_{pa} + E_{pc})/2$.²¹ The reduction of the free-base porphyrines was also studied in THF using stationary voltammetry on dropping mercury electrodes and on platinum rotating disk electrodes. Two reduction steps were detected over the available potential range (Figure 2 and Tables 1-3).

Exhaustive coulometric reductions were carried out on these same four free-base porphyrines. THF was chosen as the solvent because we expected the one-electron-reduced porphyrines, i.e., radical anions, to be stabilized in this solvent. These exhaustive reductions had to be carried out in the absence of oxygen to preclude reaction between the reduced porphyrine product and oxygen. Therefore, the electrolyses (first reduction step) were carried out under argon in a "plastic bag" glovebox. Under these conditions, the measured *n* values (faradays/mol) were then found

(21) Bard, A. J.; Faulkner, L. R. *Electrochemical Methods*; John Wiley & Sons: New York, 1980; Chapter 6.

Table 1. Half-Wave ($E_{1/2}$) Reduction Potentials of Porphycenes in THF + 0.1 M TBAP Obtained by Polarography and RDE (Volts vs SCE)^a

	RDE results		polarographic results	
	1st red.	2nd red.	1st red.	2nd red.
H ₂ Pc	-0.67 (77)	-1.0 ^b	-0.71 (60)	-1.07 (60)
H ₂ TPrPc	-0.82 (88)	-1.11 (73)	-0.85 (60)	-1.19 (70)
H ₂ OEPc	-0.84 (53)	-1.16 (90)	-0.84 (60)	-1.15 (75)
H ₂ TPrTBrPc	c		-0.38 (58)	-0.59 (55)

^a Ferrocene was oxidized at +0.55 V/SCE; it was used as internal standard. The values in parentheses are the slopes in mV of plots of E vs $\log [I/(I_d - I)]$. ^b Broadened wave. ^c Poorly resolved, broadened reduction wave.

to be close to 1. For instance, for the first reduction of H₂TPrPc, a value of $n=1.4$ faradays/mol was measured directly under these conditions. Likewise, analysis of the $\log(I)$ vs time plot of the experimental coulometric curve showed a straight line for the first 1000 s of a 2000-s electrolysis. An extrapolation of this linear segment to 2000 s then allowed a determination of $n = 1.1$ faradays/mol under conditions when no chemical reaction interfered. In addition, when this electrolytic reduction was interrupted, the solution reverted within 2–3 h in the glovebox, or within 5 min when exposed to oxygen, to the initial solution containing the unreduced porphycene. In this case, unambiguous identification of the regenerated porphycene products resulted from a combination of steady-state voltammetric and UV–vis spectroscopic analyses. Surprisingly, these oxidative regeneration reactions occurred in nearly quantitative yields. These results indicate that such a direct oxidation competes favorably with any O₂-induced decomposition pathway. A similar homogeneous process between O₂ and radical anions of aromatic hydrocarbons has been observed previously.²²

The above experimental results are consistent with a first reduction step involving the addition of one electron to the porphycene ligand. These results are further in line with those obtained by comparing the reduction-limiting currents for porphycenes and for ferrocene in steady-state voltammetry.

The high reactivity of one-electron-reduced porphycenes toward molecular oxygen was not observed with one-electron reduced free-base porphyrins. For instance, under the same experimental conditions and using the same “plastic bag” glovebox, the first reduction of H₂TPP (TPP stands here for *meso*-tetraphenylporphyrin) indicated 1.1 faradays transferred to the porphyrin, while the plot $\log(I)$ vs time was linear. H₂TPP was chosen here for comparison, rather than H₂OEP (octaethylporphyrin), because the reduction potentials of H₂TPP were close to those of the studied free-base porphycenes. In contrast herewith, H₂OEP was reduced at more negative potentials.

ESR measurements were taken on a frozen (77 K) reduced (1 faraday/mol) solution of H₂TPrPc in THF: Only a single line was observed at $g = 2.0029$. The peak to peak line width was 8.6 G. The signal observed was typical of a radical anion involving the π electron system of the porphycene. These results were fully consistent with previous studies on porphycene radicals¹³ generated by chemical reduction.

Solutions of H₂TPrPc were also subject to exhaustive reduction using sodium amalgam. In all cases, the resulting solutions exhibited properties identical to those obtained after a one-electron electrochemical reduction. Thus, the products obtained in both cases were assigned as being the anion radical H₂TPrPc^{-•}. To our surprise, all attempts at further exhaustive reduction failed. Neither electrolysis at the plateau potential of the second reduction step nor addition of excess sodium amalgam proved effective for the generation of porphycene dianions. Similar behavior was

observed in the reductions of porphyrins³ and of aromatic hydrocarbons²³ unless ultradry media were used.

Cyclic voltammetric studies were also carried out in DMF and CH₂Cl₂. They indicated that the various substituted and unsubstituted free-base porphycenes could be reduced in two distinct one-electron steps in these solvents. Each of these two steps was quasi-reversible on the time scale of cyclic voltammetry: the reduction (I_{pc}) and oxidation (I_{pa}) peak currents were proportional to the square root of the scan rate and to the concentration of the studied porphycenes; the ratio I_{pa}/I_{pc} was unity at all scan rates; the measured difference between the reduction/oxidation peak potentials was close to 58 mV for each step at low scan rates, and furthermore this peak potential separation increased with scan rate.

In CH₂Cl₂, cyclovoltammetric studies revealed two distinct oxidation steps for H₂TPrPc and for H₂OEPc. On the other hand, only one oxidative step was seen for H₂Pc (Table 2). This oxidation of H₂Pc was irreversible, and the shape of the corresponding reduction peak in cyclic voltammetry was reminiscent either of a redissolution process or of the removal of a strongly adsorbed film from the electrode surface (Figure 2a). By contrast, the first oxidation of H₂TPrPc was found to be reversible. The second oxidation process for this species was only observed on the short time scale of fast cyclic voltammetry (Figure 2b,c). Contrary to this behavior, the first oxidation peaks of H₂OEPc and H₂TBrTPrPc were irreversible at low sweep rates but became reversible at scan rates higher than 1 V/s (Figure 2f,h). Such behavior likely results from the nucleophilic attack of residual water on the electrogenerated species: indeed measurements carried out on H₂TPrPc in ultradry media exhibited two reversible oxidation steps.²⁴

Thin-layer spectroelectrochemical measurements were carried out on an OTTLE (optically transparent thin-layer electrode) in order to characterize the spectral changes associated with the oxidation and reduction reactions. As documented in Figure 3, the electrochemical conversion of the neutral porphycene H₂TPrPc to the one-electron-reduced species (Figure 3a) revealed well-defined isosbestic points, as expected for two species in equilibrium. The final spectrum is identical to that of the radical anion generated by chemical or electrochemical reduction. Further reduction of the radical anion by electrolysis at -1.2 V/SCE (Figure 3b) revealed also well-defined isosbestic points. The generated species can be oxidized stepwise back to the anion radical at -0.9 V/SCE and to H₂TPrPc at -0.7 V/SCE. Such behavior is in agreement with the generation, after a two-electron transfer, of the dianion H₂TPrPc²⁻. On the other hand, the observed spectrum of the direduced species (absence of any absorbance above around 400 nm) is similar to the spectrum of the tetraphenylbacteriochlorin dianion.²⁵ Similar spectral patterns were observed in the stepwise reductions of H₂Pc (Figure 4a), H₂OEPc (Figure 4b), and H₂TPrTBrPc (Figure 4c).

The first oxidation of H₂TPrPc was also observed on the OTTLE in CH₂Cl₂. As shown in Figure 3c, nice isosbestic points were observed during oxidation, and the generated species could be reduced back to H₂TPrPc by electrolysis at +0.9 V/SCE. These facts are consistent with the generation of a stable radical cation in this observed electrochemical oxidation step. For the reasons explained above, the corresponding dication was not observable on the time scale of stationary voltammetry.

Thus, the redox behavior of the free base porphycenes may be summarized by the following scheme which is similar to that usually proposed for porphyrins:³

(22) Santhanam, K. S. V.; Bard, A. J. *J. Am. Chem. Soc.* **1966**, *88*, 2669–2675.

(23) Peover, M. E. In *Electroanalytical Chemistry, A Series of Advances*; Bard, A. J., Ed.; Marcel Dekker: New York, 1967; Vol. 2, pp 1–51.
 (24) Lausmann, M. Unpublished results, Ph.D. Dissertation, Köln, 1993.
 (25) Peychal-Heiling, G.; Wilson, G. S. *Anal. Chem.* **1971**, *43*, 550–556.

Table 2. Potentials ($E_{pa} + E_{pc}$)/2 of Porphycenes and Metalloporphycenes Obtained on a Pt Electrode in $\text{CH}_2\text{Cl}_2 + 0.1 \text{ M TBAP}$ (V/SCE)^a

	oxidation		metal	reduction	
	2nd	1st		1st	2nd
H ₂ TPrPc	+1.44 ^c	+0.97 ^c		-0.90	-1.27
CuTPrPc ^b	+1.18	+0.88		-0.97	-1.32
NiTPrPc	+1.34	+0.90		-0.99	-1.36
CoTPrPc	+1.22	+0.99	+0.67 (II ⇌ III)	-0.99	-1.36
PtTPrPc ^b		+0.91		-0.86	-1.27
PdTPrPc ^b		+0.88		-0.89	-1.28
(FeTPrPc)O ₂ CCF ₃ ^b	+1.35	+1.13	-0.31 (III → II)	-0.94	-1.30
(FeTPrPc)Cl	+1.36	+1.13	-0.30 (III ⇌ II)	-0.92	-1.29
(AlTPrPc)Cl ^b	+1.21	+1.04		-0.82	-1.10
(MnTPrPc)Cl ^b	+1.52	+1.23	-0.42 (III ⇌ II)	-1.19	-1.55
(SnTPrPc)Cl ₂ ^b				-0.45	-0.73
H ₂ Pc		+1.0		-0.73	-1.07
H ₂ TPrPBrPc		+1.22		-0.56	-0.79
H ₂ OEPc	+1.10 ^c	+0.87 ^c		-0.94	-1.26
NiOEPc	+1.12	+0.81		-1.06	-1.41
ZnOEPc ^b	+0.78	+0.64		-1.09	-1.38
NiTPrPc-9,10,19,20	+1.05	+0.81		-0.81	-1.05
(FeTPrPc) ₂ O	+1.35; +1.20	+0.97; +0.74	-1.01 (III/III ⇌ III/II)	-1.14	-1.70 ^d

^a The above potential values were measured using cyclic voltammetry ($v = 0.1 \text{ V}\cdot\text{s}^{-1}$). Ferrocene, used as an internal standard, was oxidized at 0.48 V/SCE. ^b Potentials from ref 10. ^c Potentials at $v = 5 \text{ V}\cdot\text{s}^{-1}$. ^d Irreversible reduction peak.

Table 3. Potentials ($E_{pa} + E_{pc}$)/2 for Porphycenes and Metalloporphycenes Obtained on a Pt Electrode in DMF + 0.1 M TEAP (V/SCE)^a

	metal	ligand reduction	
		1st	2nd
H ₂ TPrPc		-0.83	-1.15
CuTPrPc		-0.87	-1.21
NiTPrPc ^b		-0.90	-1.24
CoTPrPc	+0.31 (II → III)	-0.91	-1.25
PtTPrPc ^b		-0.81	-1.16
PdTPrPc ^b		-0.83	-1.19
(FeTPrPc)O ₂ CCF ₃	-0.13 (III ⇌ II)	-0.89	-1.19
(FeTPrPc)Cl	-0.25 (III → II)	-0.89	-1.19
(AlTPrPc)Cl ^b		-0.78	-1.07
(MnTPrPc)Cl ^b	-0.32 (III ⇌ II)	-1.05	-1.33
Sn(TPrPc)Cl ₂ ^b		-0.38	-0.59
H ₂ Pc		-0.67	-0.99
H ₂ OEPc		-0.82	-1.09
NiOEPc		-0.96	-1.28
ZnOEPc ^b		-1.04	-1.35
NiTPrPc-9,10,19,20		-0.74	-0.99
(FeTPrPc) ₂ O	-0.87 (III/III ⇌ III/II)	-0.98	-1.47, -1.65 ^c

^a The above potential values were measured using cyclic voltammetry ($v = 0.1 \text{ V}\cdot\text{s}^{-1}$). Ferrocene, used as an internal standard, was oxidized in DMF + 0.1 M TEAP at +0.49 V/SCE. ^b Potentials from ref 10. ^c Detected only on a Hg electrode.



Redox Properties of the Divalent Metalloporphycenes MTPPrPc (M = Ni, Co), NiTPrPc-9,10,19,20, and NiOEPc. Cyclic voltammetric studies indicated that all four of these M(II) porphycenes were reduced via two well-separated, reversible one-electron transfers (Tables 2 and 3). The cyclic voltammograms also clearly revealed that two oxidation steps occurred for the Ni(II) porphycenes (Figure 5), whereas three distinct reversible oxidative processes took place in the case of Co^{II}TPrPc (Figure 6a). For NiTPrPc, the first oxidation peak was broader than expected for a reversible one-electron transfer reaction. Such a broadening is ascribed to an electrode surface reaction following the first oxidation step. This interpretation was confirmed by the observation that the associated reduction peak had a shape characteristic of a redissolution when the concentration of the porphycene was increased.

The oxidation of Co^{II}TPrPc deserves special mention. This porphycene exhibits one additional oxidation step when compared either to H₂TPrPc or to several other M^{II}TPrPc (M = Cu, Ni, Pd, Pt) metalloporphycenes (Tables 2 and 3). As shown in Tables 2 and 3, the first oxidation potential of Co^{II}TPrPc was shifted toward positive potentials in CH_2Cl_2 when compared to those in DMF. Such a shift in nonbonding solvents like CH_2Cl_2 is indicative of a metal-centered charge transfer as observed previously for Co^{II}TPP.²⁶ In particular, electronic absorption spectrophotometry on an OTTE indicated that the first oxidation of Co^{II}TPrPc resulted in only slight spectral changes (modest red shifts of the Soret band from 382 to 388 nm and of the Q band from 592 to 614 nm and no dramatic changes in the absorbances) (Figure 7a). By contrast, the spectral changes associated with the second oxidation of Co^{II}TPrPc (Figure 7b) were found to be similar to those observed during the first oxidation of either Ni^{II}TPrPc or Ni^{II}OEPc (Figure 8a,b). These results lead us to conclude that the first oxidation process for Co^{II}TPrPc corresponds to a metal-centered electron transfer in the Co(II)/Co(III) couple, rather than to a redox process involving the ligand porphycene framework. If such an assignment is correct, one would expect the second and the third oxidation steps to correspond to redox changes at the porphycene ligand, generating successively the monoradical cation and the dication and leading to the associated characteristic spectral changes. This indeed was observed by experiments (compare for instance Figure 7b with Figure 8a,b).

Exhaustive electrochemical reductions of these metalloporphycenes, in THF at potentials corresponding to their first reduction, confirmed that one electron was being transferred. In fact, the UV-vis absorption spectra of the resulting solutions were quite similar to those obtained after the first reduction of the free bases. Furthermore, the ESR spectra of frozen solutions of the one-electron reduced metalloporphycenes exhibited a single signal with $g = 2.0036$ (peak to peak line width 8.16 G) for the nickel porphycene and $g = 2.0031$ (peak to peak line width 8.99 G) for the cobalt porphycene. This is consistent with the presence of a radical anion. ESR spectra of radical anions of nickel porphycenes have been studied extensively^{9,13b} and exhibited signals similar to those reported above. Thus, for the cobalt porphycene, the overall electrochemical behavior is very much different from that of cobalt(II) porphyrins, in which the cobalt-

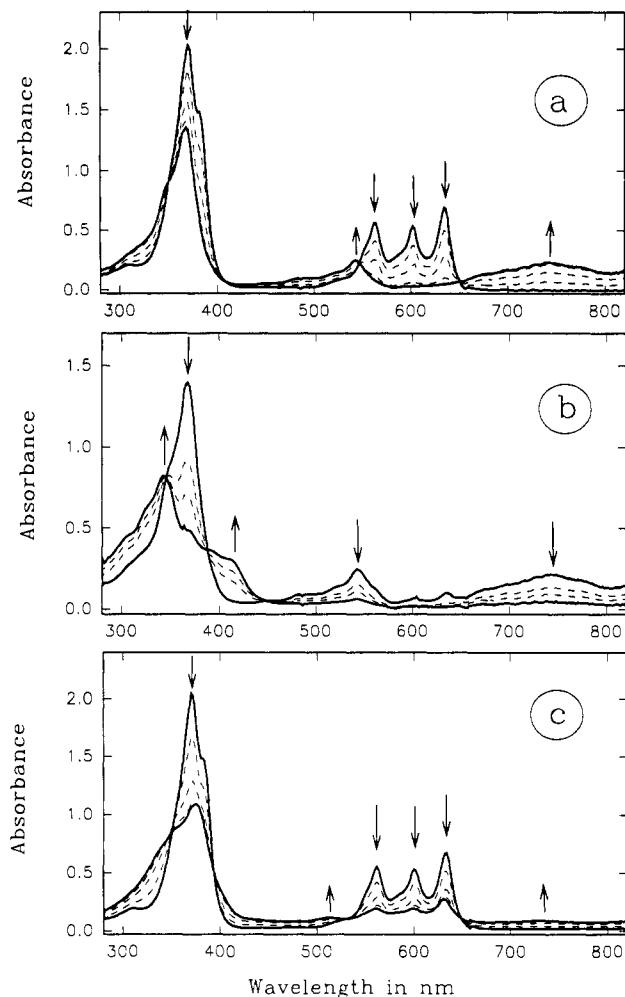


Figure 3. Time-resolved UV-vis spectra for the reduction of H_2TPrPc in $THF + 0.1 M TBAP$ on an OTTLE: (a) first reduction step at a controlled potential of $-0.9 V$; (b) second reduction step at a controlled potential of $-1.2 V$; (c) first oxidation step at a controlled potential of $+1.1 V$ (recorded in $CH_2Cl_2 + 0.1 M TBAP$).

(II) center is often reduced to cobalt(I) before the reduction of the ligand occurs.^{27,28}

As already observed for the free-base porphycenes, two-electron-reduced species could not be generated on the time scale of exhaustive coulometries for these metal porphycenes. This was true whether the attempted double reduction was carried out using either an excess of sodium amalgam or exhaustive reductive electrolysis. However, the reduction of the metalloporphycene radical anions to the corresponding dianions was easily carried out with an OTTLE approach because it involves shorter time scales. Here, the electrolytic reductions exhibited well-characterized absorption spectra with nice isosbestic points. Thus, it is tempting to conclude that doubly reduced metalloporphycene species can be produced but that such species are likely very unstable.

Electrochemistry of $(Fe^{III}TPrPc)Cl$ and $(Fe^{III}TPrPc)_2O$. The redox properties of the mononuclear iron(III) porphycenes were analyzed using a combination of standard cyclic voltammetry and OTTLE-type absorption spectroscopy. This combination was expected to facilitate the observation of electrogenerated species. In the event, cyclic voltammograms of $(Fe^{III}TPrPc)Cl$ exhibited five distinct redox steps in CH_2Cl_2 (Table 2), namely three reductions and two oxidations, as illustrated in Figure 6b.

(27) Kadish, K. M.; Lin, X. Q.; Han, B. C. *Inorg. Chem.* **1987**, *26*, 4161-4167.

(28) (a) Whitlock, H. W.; Bower, B. K. *Tetrahedron Lett.* **1965**, 4827-4831. (b) Momenteau, M.; Fournier, M.; Rougée, M. *J. Chim. Phys. Phys.-Chim. Biol.* **1965**, *67*, 926-933.

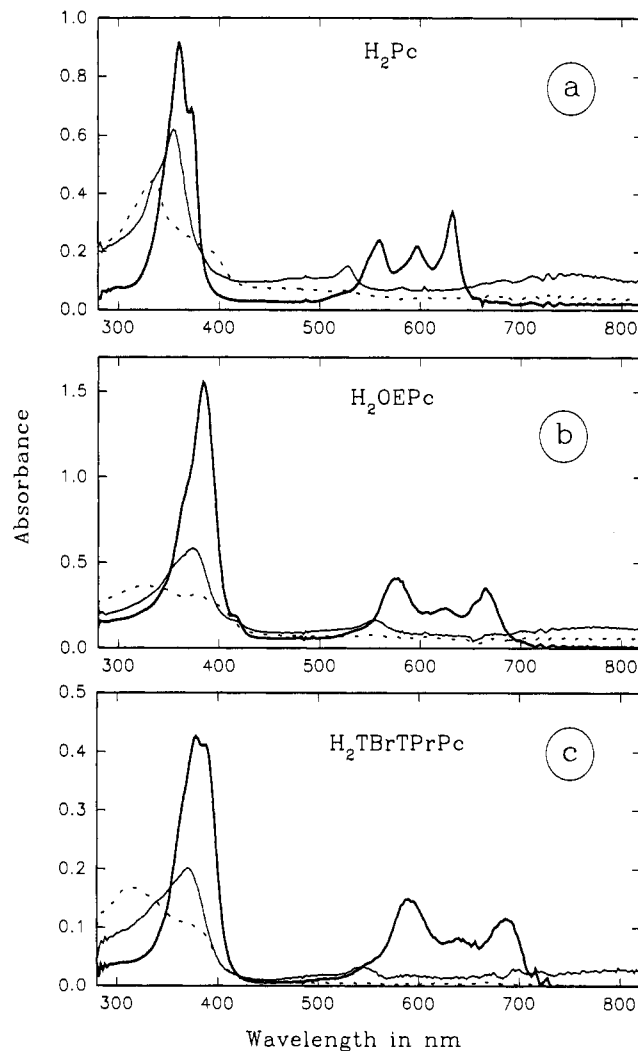


Figure 4. UV-vis absorption spectra of the free base porphycenes and their reduced species. (a) UV-vis spectra in CH_2Cl_2 on an OTTLE: H_2Pc (—), electrogenerated $H_2Pc^{\bullet-}$ (—), $H_2Pc^{2\bullet-}$ (---). (b) UV-vis spectra in THF on an OTTLE: H_2OEPc (—), electrogenerated $H_2OEPc^{\bullet-}$ (—), $H_2OEPc^{2\bullet-}$ (---). (c) UV-vis spectra in THF on an OTTLE: $H_2TBrTPrPc$ (—), electrogenerated $H_2TBrTPrPc^{\bullet-}$ (—), $H_2TBrTPrPc^{2\bullet-}$ (---).

In DMF, by contrast, only the three reduction steps were observed. The first reduction had the characteristics of a reversible one-electron transfer on the time scale of cyclic voltammetry. On the other hand, the associated reoxidation step exhibited a broad peak at low sweep rates ($v < 1 V \cdot s^{-1}$), while two distinct peaks were observed at higher sweep rates. Further, when chloride anions (as $(TBA)Cl$) were added to solutions containing the porphycene and TBAP as the conducting electrolyte, this reoxidation reaction was represented at all sweep rates by a single peak which had the characteristics of a reversible transfer, as observed previously with iron(III) porphyrins.^{29,30} Thus, the first one-electron reduction of $(Fe^{III}TPrPc)Cl$ can be characterized as being an EC process, in which a reversible electron transfer (E) is followed by a reversible chemical step (C). The other four redox steps (i.e. two further reductions and two oxidations) were reversible at scan rates lower than $1 V \cdot s^{-1}$ and became quasi-reversible at higher scan rates. Stepwise reduction of $(Fe^{III}TPrPc)Cl$ on an OTTLE led to well-defined spectral patterns (Figure 9). Each reduction step exhibited absorption spectra with well resolved isosbestic points. When compared with those observed for free-base porphycenes (Figure 3) and for other metallo(II)porphycenes, the observed spectra (Figure 9) are

(29) Bottomley, L. A.; Kadish, K. M. *Inorg. Chem.* **1981**, *20*, 1348-1357.

(30) Maiya, B. G.; Mallouk, T. E.; Hemmi, G.; Sessler, J. L. *Inorg. Chem.* **1990**, *29*, 3738-3745.

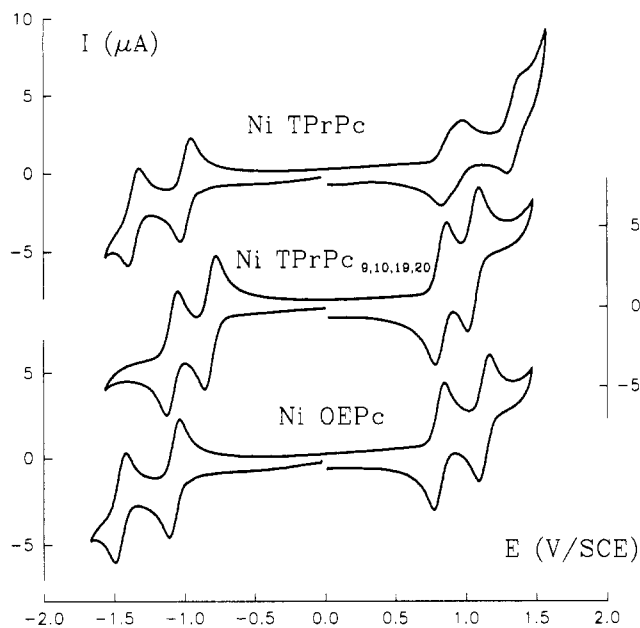


Figure 5. Cyclic voltammograms of nickel(II) porphycenes on Pt electrodes at 0.1 V/s in $\text{CH}_2\text{Cl}_2 + 0.1 \text{ M TBAP}$.

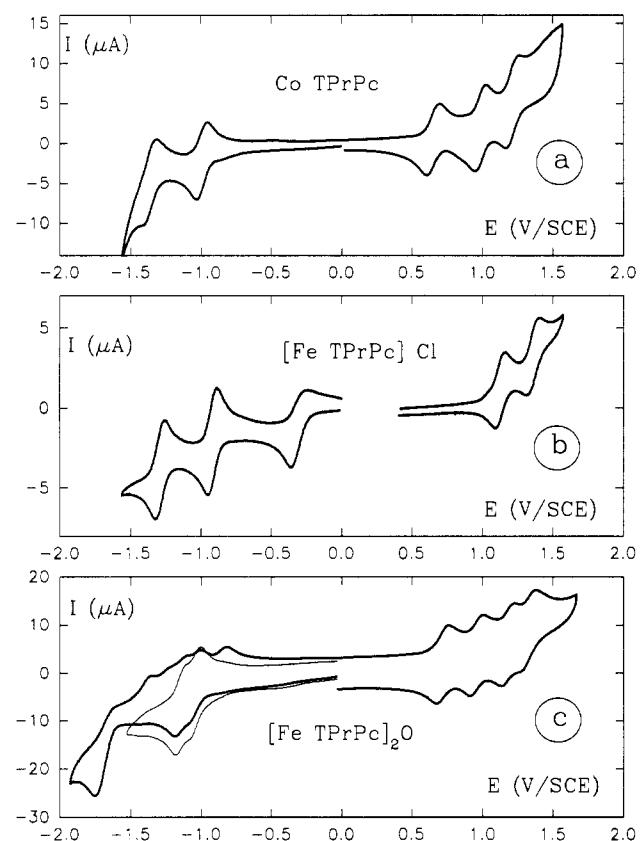
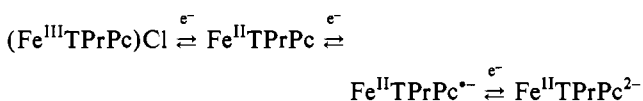


Figure 6. Cyclic voltammetry in $\text{CH}_2\text{Cl}_2 + 0.1 \text{ M TBAP}$ on (a, b) a Pt electrode and on (c) a GC electrode.

considered consistent with the following reduction scheme:



When $(\text{Fe}^{\text{III}}\text{TPrPc})\text{Cl}$ was reduced exhaustively at the plateau potential corresponding to the first reduction step (reduction of Fe(III) to Fe(II)), the corresponding iron μ -oxo porphycene resulted. It was identified by its UV-vis absorption spectrum and its electrochemical behavior. Thus, under the experimental

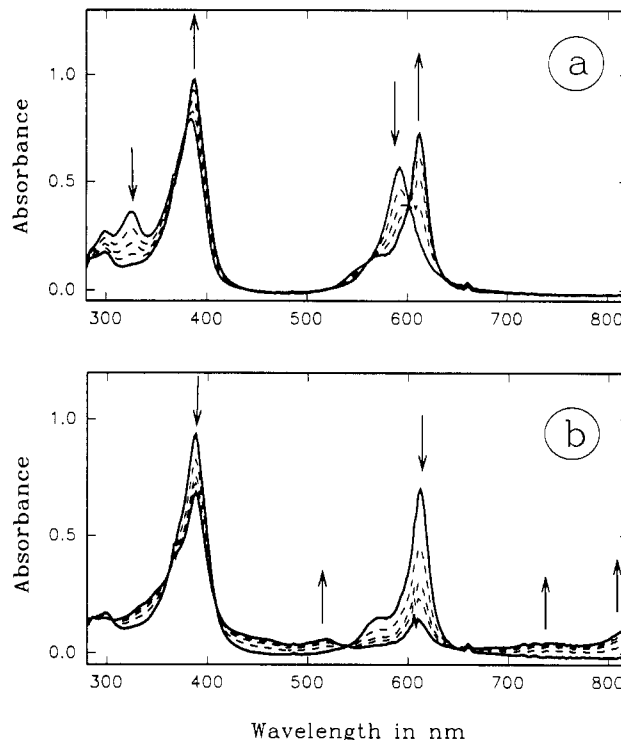


Figure 7. Time-resolved UV-vis spectrum for the oxidation of $\text{Co}^{\text{II}}\text{TPrPc}$ in $\text{THF} + 0.1 \text{ M TBAP}$ on an OTTLE: (a) at a controlled potential of +0.7 V, first oxidation step; (b) at a controlled potential of +1.0 V, second oxidation step.

conditions of this exhaustive coulometry, traces of oxygen in the solution precluded the generation of any observable monomeric iron(II) species.

The electrochemical oxidation of $(\text{Fe}^{\text{III}}\text{TPrPc})\text{Cl}$ was also studied. Under OTTLE conditions the species generated by the first oxidation (Figure 8c) had the spectrum of a metalloporphycene radical cation (typified, for instance, by the spectrum in Figure 7b or that of a radical cation generated from free-base porphycenes (Figure 3c)). These observations indicated that the generated species was likely the radical cation, i.e. $\text{Fe}^{\text{III}}\text{TPrPc}^{\cdot+}$, although the generation of iron(IV) cannot be fully ruled out. Moreover, studies of a series of iron(III) porphycenes with different axial anionic ligands ($\text{XFe}^{\text{III}}\text{TPrPc}$ where $\text{X} = \text{Cl}, \text{Br}, \text{N}_3$)²⁴ showed that the first oxidation potential was not influenced by axial ligation to the iron. Such behavior is an additional indication of a ligand-centered oxidation process rather than a metal-centered electron transfer.³¹

The electrochemical behavior of the iron μ -oxo derivative $(\text{Fe}^{\text{III}}\text{TPrPc})_2\text{O}$ was also analyzed. This dinuclear species underwent up to eight distinct electron transfers, thus corresponding to nine different redox states. Four of those reactions were reversible one-electron oxidations, as documented in Table 2 and in Figure 6c. In CH_2Cl_2 on a Pt or glassy carbon electrode, or in DMF on a platinum electrode, three reduction steps were observed. The first two reductions overlapped and were reversible on the time scale of cyclic voltammetry. The third reduction step changed from a two-electron irreversible reduction at scan rates lower than 1 V/s to a one-electron reversible reduction at higher scan rates. On a mercury electrode four distinct reductions were observed in DMF. They were reversible on a cyclic voltammetric time scale of 5–50 V/s. However, strong adsorption of the reacting species on the mercury electrode in the two first reductions enhanced the signals. In DMF, and on Hg, the measured values for $(E_p + E_p)/2$ were –0.86, –1.06, –1.47, and –1.65 V/SCE, respectively.

(31) Phillipi, M. A.; Shimomura, E. T.; Goff, H. M. *Inorg.Chem.* **1981**, *20*, 1322–1325.

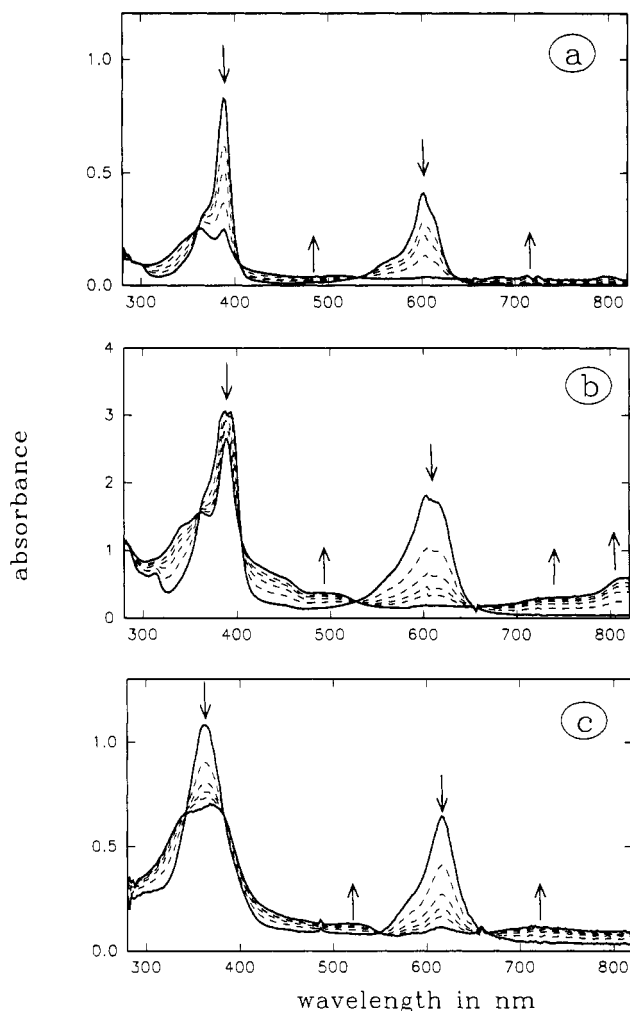


Figure 8. Time-resolved UV-vis absorption spectra of Fe(III) and Ni(II) porphycenes and of their one-electron-oxidation products on an OTTLE in $\text{CH}_2\text{Cl}_2 + 0.1 \text{ M TBAP}$. (a) $\text{Ni}^{\text{II}}\text{TPrPc}$, electrolysis at +1.20 V; (b) $\text{Ni}^{\text{II}}\text{OEPC}$, electrolysis at +1.00 V; (c) $\text{Fe}^{\text{III}}\text{TPrPc}$, electrolysis at +1.25 V.

Using Pt-OTTLE spectroscopy in DMF, it was found that the μ -oxo dimer ($\text{Fe}^{\text{III}}\text{TPrPc}$)₂O exhibits well defined isosbestic points while undergoing the first reduction step (Figure 10a). This was taken as an indication that there are no detectable intermediate chemical species between the starting bis(ferric) species and its resulting monoreduced form. Indeed, the spectral changes associated with this reaction (only a slight decrease of the Q band at $\lambda = 632 \text{ nm}$ and an inversion in the intensities of the twinned Soret bands from 344 (sh) and 368 nm to 342 and 362 nm (sh)) suggest that this first observed reduction does not perturb substantially the interaction between the two ligands. Thus, although conclusive evidence remains awaited, these results suggest that the first reduction might occur here on one iron(III), thus generating a mixed-valence bis(porphycene) $\text{Fe}^{\text{III}}\text{TPrPc-O-Fe}^{\text{II}}\text{TPrPc}$. In contrast to the above, the second reduction step was found to yield an absorption spectrum (Figure 10b) typical of anion radicals (compare, for instance, with Figure 3a and Figure 9b). However, the spectrum of the direduced species was not identical with that observed for the mononuclear iron(II) radical anion. So it is likely that the dinuclear species was not destroyed during reduction. Moreover the initial spectrum of the μ -oxo dimer was restored after stepwise oxidations. More detailed studies on the redox reactions of this iron μ -oxo are underway.

Discussion

The present electrochemical results indicate that porphycene

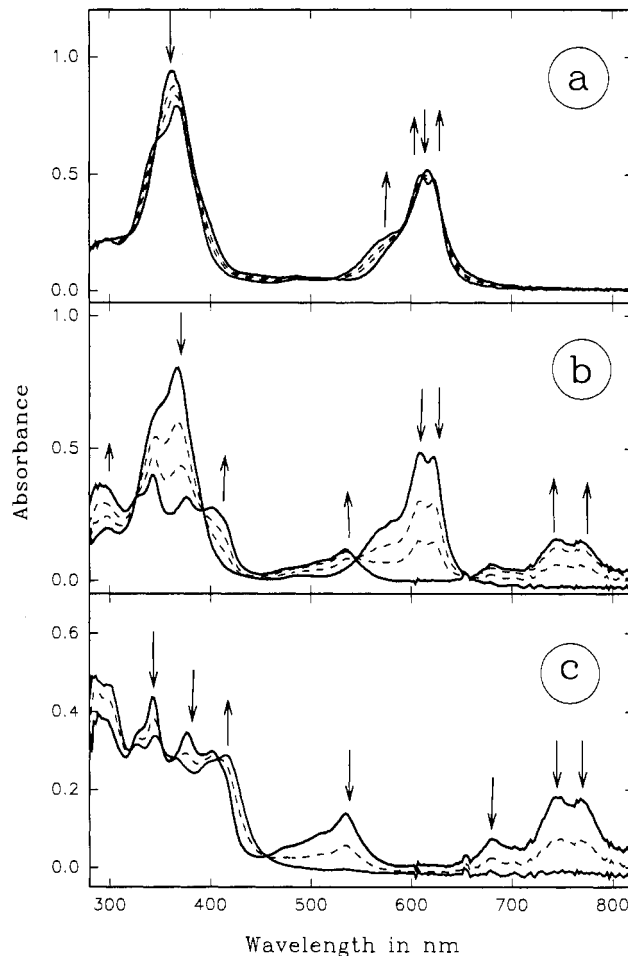


Figure 9. Time-resolved UV-vis spectra for the reduction of ($\text{Fe}^{\text{III}}\text{TPrPc}$)-Cl in THF + 0.1 M TBAP on an OTTLE: (a) first reduction step at a controlled potential of -0.5 V; (b) second reduction step at a controlled potential of -1.0 V; (c) third reduction step at a controlled potential of -1.4 V.

free bases undergo, on the available potential range (up to -2.7 V/SCE), only two one-electron reductions of the porphycene ring system in all studied solvents. This is at variance with the known behavior of the porphyrin free-bases, which exhibit a total of four distinct reductions.^{25,32-34} Porphycene free bases are reduced in DMF at potentials less negative (-0.83 V/SCE for H_2TPrPc and -0.82 V/SCE for H_2OEPC) than those for the corresponding porphyrin free bases (-1.43 V/SCE for H_2OEP), whereas oxidations occur at about the same potentials in CH_2Cl_2 (+0.97, +0.87, and +1.02 V/SCE for H_2TPrPc , H_2OEPC , and H_2OEP , respectively). These results suggest that the energy of the LUMO orbitals is lower in the porphycenes than in the porphyrins. In addition, it was also observed that, under the above described experimental conditions, large-scale exhaustive electrolytic reduction of the free-base porphycenes was difficult to carry out. This could be due to solvent impurities (traces of water and oxygen) that react with the generated species. Such behavior is well-known for aromatic hydrocarbons²³ as well as for porphyrins³ owing to the strong basicity of the-generated species. In the case of porphyrins, reduction often yielded chlorins or phlorins as final products instead of the dianion.³ The purpose of the present work was to identify as far as possible the electrogenerated species rather than to study the generated species.

(32) Cosmo, R.; Kautz, C.; Meerholz, K.; Heinze, J.; Müllen, K. *Angew. Chem., Int. Ed. Engl.* **1989**, *28*, 604-607.

(33) Clack, D. W.; Hush, N. S. *J. Am. Chem. Soc.* **1965**, *87*, 4238-4242.

(34) Peychal-Heiling, G.; Wilson, G. S. *Anal. Chem.* **1971**, *43*, 545-550.

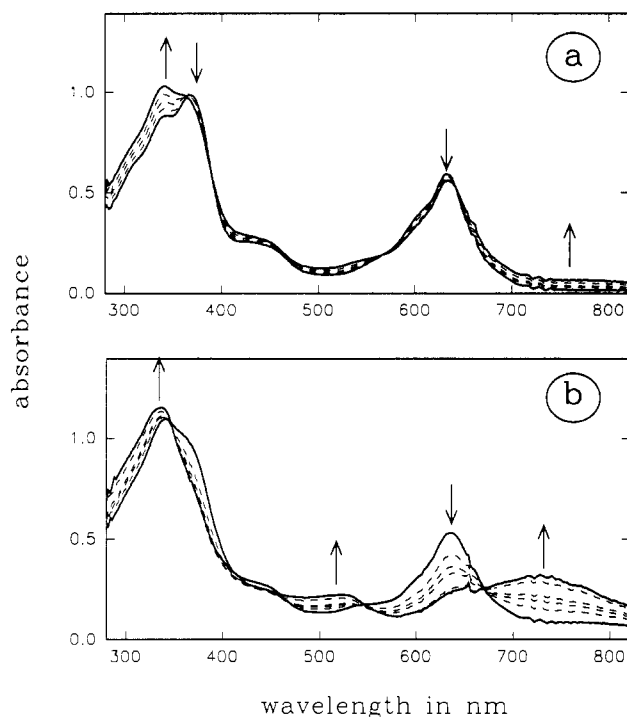


Figure 10. Time resolved UV-vis absorption spectra corresponding to (a) the first and (b) the second one-electron reductions of $(\text{Fe}^{\text{III}}\text{TPrPc})_2\text{O}$ on a Pt OTTLE in DMF + 0.1 M TBAP.

As pointed out in the literature,³⁵ for the latter purpose, chemical reduction by a sodium mirror under clean conditions on a vacuum line avoids many subsequent side reactions often observed in electrochemical reductions. Be that as it may, the above results clearly illustrate the exceptionally high trend of the reduced free-base porphycenes to rearomatize, i.e. to revert from the one-electron reduced species to the initial molecule. In spite of this, it is interesting to notice that the radical anions and dianions have been generated and characterized on the short time scale associated with the cyclic voltammetric method. Previous studies have pointed out that the radical anions of porphycenes, obtained by chemical reduction under high-vacuum conditions, were stable for several weeks when stored at -27°C .^{13b}

Substituent Effects on the Redox Properties of Free-Base Porphycenes. For the four studied free-base porphycenes H_2Pc , H_2TPrPc , H_2OEPC , and $\text{H}_2\text{TPrTBrPc}$, the sequence of the measured oxidation and reduction potentials (Tables 1–3) qualitatively follows the order of the expected inductive effects of the substituents on the tetrapyrrolic ring system. Therefore, when compared with those of the nonsubstituted porphycene H_2Pc , these potentials were shifted to more negative values as a result of the electron-donating propyl and ethyl groups. On the other hand, electron attracting bromo substituents shifted the potentials toward more positive values. However, on the basis of any of the several Hammett σ values, no significant linear correlation could be established with these shifts in the potentials. This is in marked contrast to the additivity of inductive effects generally observed in the reduction of porphyrins.^{7,8} This failure to observe a linear correlation may be ascribed, at least in part, to steric hindrance between substituents, which leads to distortions of the ring systems of H_2OEPC ¹⁴ and $\text{H}_2\text{TPrTBrPc}$.^{18b}

In addition to the above results, other molecular properties reflected the differences in reactivity between H_2TPrPc and H_2OEPC as a result of the nonplanarity of the latter. For instance, when changes in the UV-vis absorption spectra of H_2TPrPc and H_2OEPC were monitored as a function of time in DMF while HClO_4 was added in large excess (acid/porphycene molar ratio

of 100), the absorption spectrum of H_2TPrPc remained unchanged for hours. By contrast, the absorption spectrum of H_2OEPC changed slowly with time, exhibiting a decrease in the Soret band at 386 nm while a new band was seen to increase at 410 nm. This reactivity difference may be rationalized by the strong $\text{N-H}\cdots\text{N}$ hydrogen bonding¹⁵ observed in H_2TPrPc and in H_2Pc , which renders protonation more difficult. The nonplanarity of H_2OEPC , on the other hand, serves to keep the inner cavity open and, thus, makes the nitrogen more accessible to protonation.

It is of interest to compare the protonation behavior of H_2TPrPc with that of H_2TPP . Under the same 100-fold excess of HClO_4 , the porphyrin H_2TPP was protonated in 0.5 h, whereas no detectable protonation of the porphycene H_2TPrPc was observed. Actually, H_2TPrPc was only protonated when an extremely high excess of HClO_4 (beyond 60 000 fold excess) was used.

Substituent Effects on the Redox Properties of Nickel(II) Porphycenes. The Ni(II) porphycenes provide a convenient congruent set for documenting substituent effects. $\text{Ni}^{\text{II}}\text{TPrPc}$ was one of the first M(II) porphycenes to be studied electrochemically.⁹ Recently, the structural characteristics and the physicochemical properties of diverse sets of substituted Ni(II) porphycenes became known.^{2,13b,17,18a}

The measured redox potentials (Figure 5 and Tables 2 and 3) indicate that the difference between the $(E_{\text{p}_1} + E_{\text{p}_2})/2$ potentials corresponding to the first oxidation and the first reduction was significantly smaller for $\text{NiTPrPc-9,10,19,20}$ ($\Delta E = 1.62\text{ V}$) than for NiOEPC ($\Delta E = 1.87\text{ V}$) or NiTPrPc ($\Delta E = 1.89\text{ V}$). Thus four ostensibly similar propyl substituents cause a greater decrease in the value of ΔE when they are located in positions 9, 10, 19, and 20 on the porphycene periphery than when they are found in positions 2, 7, 12, and 17. The smaller ΔE for $\text{NiTPrPc-9,10,19,20}$, as compared with those of NiOEPC and NiTPrPc , is mirrored in a greater red shift observed in the UV-Vis spectrum of this species as compared to those of the other porphycenes. This is true for both the α and the Soret bands. In CH_2Cl_2 , for instance, the band (λ_{max}) occurs at 644 nm for $\text{NiTPrPc-9,10,19,20}$ but only at 602 and 604 nm for NiOEPC and NiTPrPc , respectively. Likewise, the Soret band (λ_{max}) of this material is observed at 394 nm as compared to 386 nm for NiOEPC and 388 nm for NiTPrPc .

We interpret the above substituent effects as resulting mainly from the distortion of the porphycene ring system induced by the propyl groups in $\text{NiTPrPc-9,10,19,20}$.^{18a} Such an interpretation is consistent with prior X-ray structural work wherein "a maximum distance of 0.45 Å was observed from the best plane through the porphycene skeleton and the nickel atom" for this system whereas little distortion was seen for the corresponding 2,7,12,17-substituted isomer.^{18a} The simultaneous facilitation of the first reduction and oxidation steps in this Ni(II) porphycene thus parallels the expected decrease in the energy gap between the HOMO and LUMO orbitals linked to changes in spectral properties and in conformational geometry.^{36,37} Although, in this porphycene, the propyl groups likely exert inductive effects on the energy of these orbitals, it is clear from the experimental results that the distortion effects are predominant.

Iron(III) μ -Oxo Porphycene. The above-reported electrochemical behavior of this dinuclear species in CH_2Cl_2 was compared with that of the iron(III) porphyrin analog $(\text{Fe}^{\text{III}}\text{TPP})_2\text{O}$. Previous studies^{38–40} demonstrated that $(\text{Fe}^{\text{III}}\text{TPP})_2\text{O}$ was oxidized in three one-electron reversible steps at potentials

(35) Teraoka, J.; Hashimoto, S.; Mori, M.; Kitagawa, T. *J. Am. Chem. Soc.* **1987**, *109*, 180–184.

(36) Cotton, F. A.; Wilkinson, G. *Advanced Inorganic Chemistry*, 3rd ed.; Interscience: New York, 1972.

(37) Atkins, P. W. *Physical Chemistry*, 2nd ed.; Oxford University Press: Oxford, U.K., 1982.

(38) Cohen, I. A.; Lavalley, D. K.; Kopelove, A. B. *Inorg. Chem.* **1980**, *19*, 1100–1101.

(39) Felton, R. H.; Owen, G. S.; Dolphin, D.; Fajer J. *J. Am. Chem. Soc.* **1971**, *93*, 6332–6334.

(40) Phillippi, M. A.; Goff, H. M. *J. Am. Chem. Soc.* **1979**, *101*, 7641–7643.

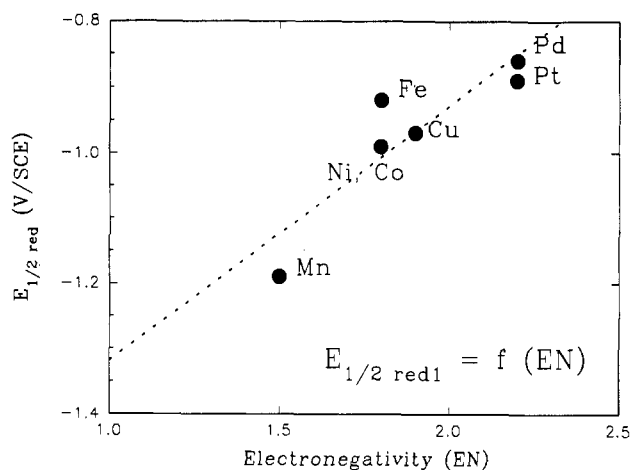


Figure 11. Redox correlations for $M^{II}TPrPc$. Plot of the first ring reduction vs electronegativity of the central divalent metal ion.

of +0.84, +1.12, and +1.50 V/SCE. This behavior is not much different from that observed here for $(Fe^{III}TPrPc)_2O$ (which underwent four distinct one-electron oxidations; vide supra and also Table 2). Although their essential oxidation behaviors are similar, $(Fe^{III}TPP)_2O$ and $(Fe^{III}TPrPc)_2O$ differ dramatically in the stability of their resulting reduction products. In either CH_2Cl_2 ³⁸ or DMF ⁴¹ solution, the porphyrin-based μ -oxo species decomposed rapidly only after the second reduction step and ultimately generated FeTPP and the corresponding anion radical. By contrast, the porphycene based μ -oxo species $(Fe^{III}TPrPc)_2O$ could be reduced in four distinct one-electron steps. The two first reductions were reversible on the time scale of cyclic voltammetry, even at low scan rates (0.01 V/s). The resulting species could then be reduced further to yield a species assigned as being, presumably, $[(FeTPrPc)_2O]^{4-}$ arising via two distinct electron transfers which were reversible at high scan rates ($v > 5 \text{ V}\cdot\text{s}^{-1}$).^{42,43} This is clearly very different from what is seen in the case of the porphyrins. Indeed, only μ -oxo Fe(III) porphyrin dimers bearing four electron attracting cyano groups exhibited a similar electrochemical behavior: four reversible reduction waves were observed⁴⁴ for this porphyrin μ -oxo dimer, just as was the case for $(Fe^{III}TPrPc)_2O$.

Redox Potentials and Metal/Ligand Interactions. For the studied $M^{II}TPrPc$ porphycenes, the first reduction potential was found to correlate well with the electronegativity of the central metal (Figure 11). This would suggest that, as is true for M(II) porphyrins,⁶ the energy of the LUMO molecular orbital (the one accepting the first electron in $M(II)TPrPc$) depends on the electronegativity of the coordinated metal M(II).

Conclusion

In comparison to those of the porphyrins, the redox properties of porphycenes differ in a number of substantial ways. For instance, in contrast to the porphyrins, the porphycenes studied

herein exhibit only two reversible one-electron reduction steps in the potential range 0 to -2.7 V/SCE . Under the same experimental conditions, however, the porphyrins are found to undergo reduction in four distinct redox steps, the last two of which are observed to be sensitive to the water content of the solvent.^{25,32-34} These last two reduction steps have no parallel in the case of the porphycenes. As a result, the redox behavior of the porphycenes is similar to that of bacteriochlorin.²⁵ This latter molecule, like the porphycenes, has a D_{2h} symmetry. In such a symmetry, calculations⁴⁵ suggest that the $e_g(\pi^*)$ molecular orbitals, degenerate in porphyrins of D_{4h} symmetry, are expected to be split. Indeed, recent studies indicate that this splitting should be substantial in the case of both bacteriochlorins (BC)⁴⁶ (ca. -1.58 eV for ZnTPBC) and porphycenes¹⁷ (splitting on the order of -1.1 to -1.4 eV). Thus, as a consequence, the third and fourth reductions of the porphycenes are predicted to lie beyond the accessible potential range (here -2.7 V/SCE).

The potential difference between the first oxidation and the first reduction, $\Delta E = E_{ox1} - E_{red1}$, remained nearly constant ($1.85 \pm 0.15 \text{ V}$) throughout the set of studied porphycenes, as previously reported.⁹⁻¹⁰ For the iron and manganese porphycenes, in which the metal was an electroactive site, the observed ΔE was higher than this characteristic value. This observed 1.85-V energy difference is significantly smaller than that routinely observed for porphyrins ($\Delta E = 2.25 \pm 0.15 \text{ V}$).⁶ If this energy difference ΔE expresses the energy gap between the most stable vacant molecular orbital (LUMO) and the least stable filled molecular orbital (HOMO) in the studied molecules, then the smaller ΔE measured for the porphycenes can again be taken as reflecting the lower symmetry present in the porphycenes. The measured ΔE for bacteriochlorins ($\Delta E = 1.50 \text{ V}$)⁴⁷ certainly supports this interpretation of a close link between the loss of symmetry and the decrease of ΔE . Further support for this conclusion is also provided by an examination of the energy differences between the first and second reductions; these are smaller in the case of the porphycenes ($0.35 \pm 0.07 \text{ V}$) than in the case of porphyrins ($0.42 \pm 0.05 \text{ V}$).⁶ Thus, it is clear that changes in symmetry play an important role in modulating the redox and optical properties of ostensibly similar, porphyrin or porphyrin-like tetrapyrrolic macrocycles.

As a final conclusion it is worth noting that, in contrast to the behavior of porphyrins^{7,8} the substituent effects were not additive in the case of porphycenes. While the lower symmetry of the porphycene tetrapyrrolic ring may reasonably contribute to this nonadditivity, there is little doubt that steric interactions also exert significant effects. This is especially obvious when a comparison is made between tetrapropylporphycenes bearing the propyl substituents either on the ethene bridges or on the pyrroles: the ΔE splitting decreased from 1.89 to 1.63 V (cf. Table 2) as a result of this isomeric change. Thus, these results highlight further the importance of symmetry, or factors that might adjust or reduce it, in defining the overall properties of the porphycenes. Such conclusions were also reached recently in the context of studies of excited triplet states of porphycenes.¹²

Acknowledgment. The authors thank Dr. J. L. Sessler for his kind assistance in the editorial process of this paper.

- (41) Kadish, K. M.; Larson, G.; Lexa, D.; Momenteau, M. *J. Am. Chem. Soc.* **1975**, *97*, 282-288.
 (42) The chemical stability of all four reduced species was good in dry solvents. Traces of water cause the decomposition of the μ -oxo dimer beyond the second reduction step (unpublished results from Prof. M. L'Her and Dr. Y. Le Mest, UBO, Brest, France).
 (43) The authors gratefully thank Prof. K. M. Kadish (University of Houston) for fruitful exchange of information on the redox behavior of μ -oxo bis(iron(III) porphycenes).
 (44) Kadish, K. M.; Boisselier-Cocolios, B.; Simonet, B.; Chang, D.; Ledon, H.; Cocolios, P. *Inorg. Chem.* **1985**, *24*, 2148-2156.

- (45) Longuet-Higgins, H. C.; Rector, C. W.; Platt, J. R. *J. Chem. Phys.* **1950**, *18*, 1175-1181.
 (46) Barkigia, K. M.; Miura, M.; Thompson, M. A.; Fajer, J. *Inorg. Chem.* **1991**, *30*, 2233-2236.
 (47) Chang, C. K.; Hanson, L. K.; Richardson, P. F.; Young, R.; Fajer, J. *Proc. Natl. Acad. Sci. U.S.A.* **1981**, *78*, 2652-2656.